

DOI: 10.1002/cmdc.200700271

A 3D QSAR Model of 17 β -HSD1 Inhibitors Based on a Thieno[2,3-*d*]pyrimidin-4(3*H*)-one Core Applying Molecular Dynamics Simulations and Ligand–Protein Docking

Sampo Karkola, Annamaria Lilienkamp, and Kristiina Wähälä*^[a]

The 17 β -hydroxysteroid dehydrogenase type 1 (17 β -HSD1) enzyme plays a crucial role in female hormonal regulation by catalysing the NADPH-dependent reduction of the less potent estrone E1 into the biologically active estradiol E2. Because 17 β -HSD1 is a key enzyme in E2 biosynthesis, it has emerged as an attractive drug target for inhibitor development. Herein we report the plausible binding modes and a 3D QSAR model of 17 β -HSD1 inhibitors based on a (di)cycloalkenothieno[2,3-*d*]pyrimidin-4(3*H*)-one core. Two generated enzyme complexes with potent inhibitors were subjected to molecular dynamics simulation to mimic the dynamic process of inhibitor binding. A set of 17 β -HSD1 in-

hibitors based on the thieno[2,3-*d*]pyrimidin-4(3*H*)-one core were docked into the resulting active site, and a CoMFA model employing the most extensive training set to date was generated. The model was validated with an external test set. Active site residues involved in inhibitor binding and CoMFA fields for steric and electrostatic interactions were identified. The model will be used to guide structural modifications of 17 β -HSD1 inhibitors based on a thieno[2,3-*d*]pyrimidin-4(3*H*)-one core in order to improve the biological activity as well as in the design of novel 17 β -HSD1 inhibitors.

Introduction

Breast cancer is the most common cancer in women in Western countries, and it has been estimated that 178 480 new cases were diagnosed in the US in 2007.^[1] Most breast tumors are initially estrogen-receptor positive, that is, hormone-dependent, and estrogens, especially estradiol (E2), have a pivotal role in their development. Controlling the levels of circulating and tissue E2 by inhibiting its biosynthesis is thus a rational approach for treating hormone-dependent breast cancers.^[2] A major class of enzymes that produce estrogens are the 17 β -HSDs.^[3] Other enzymes that generate estrogens, primarily estrone (E1), are CYP19 aromatase and steroid sulfatase. Aromatase inhibitors have already reached the market,^[4] but due to the lack of a crystal structure, homology models^[5] remain the basis for structure-based drug design.

The 17 β -hydroxysteroid dehydrogenase type 1 (17 β -HSD1) enzyme plays a crucial role in the female hormonal regulation by catalysing the NADPH-dependent reduction of the less potent E1 **1** into the biologically active E2 **2** (Figure 1). 17 β -HSD1 belongs to the short-chain alcohol dehydrogenase superfamily (SDR) and has the conserved and catalytically crucial Tyr-x-x-x-Lys sequence and a generally conserved Ser in the

active site (catalytic triad Tyr 155, Lys 159 and Ser 142 in 17 β -HSD1).^[6] Several crystal structures of 17 β -HSD1^[7] are available. The enzyme has been co-crystallised with estrogens^[8] and androgens^[9] and with two steroid based inhibitors.^[8c,10] The 17 β -HSD1 enzyme contains a loop near the active site (residues 190–200) for which several conformations have been observed in crystal structures. This loop has been associated with substrate entry. In addition to the crystallographic studies, molecular modelling^[11] has been employed to investigate the active site as well as alternative binding modes of steroids.^[12]

The human 17 β -HSD1 is active as a soluble cytosolic homodimer^[13] and is mainly expressed in ovaries, placenta and breast tissue.^[14] where it is suggested to have an important role in *in situ* E2 production.^[15] Because 17 β -HSD1 is a key enzyme in E2 biosynthesis, it has emerged as an attractive drug target for inhibitor development.^[16] Recently, *in vivo* efficacy of 17 β -HSD1 inhibition of hormone-dependent tumour growth has been demonstrated in immunodeficient mice inoculated with MCF-7 cells expressing the human recombinant 17 β -HSD1 enzyme (rec17 β -HSD1).^[17] The majority of known inhibitors of 17 β -HSD1 are based on modifications of steroidal structures, especially E1 and E2.^[16,18–24] Less work has been published regard-

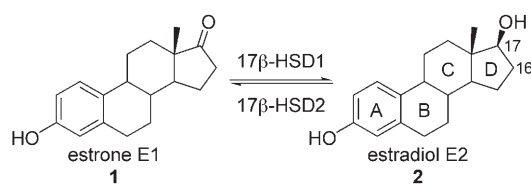


Figure 1. The primary enzymatic reaction catalysed by 17 β -HSD1, with steroid core labelling shown.

[a] S. Karkola, Dr. A. Lilienkamp,⁺ Prof. K. Wähälä
Laboratory of Organic Chemistry
Department of Chemistry, University of Helsinki
PO Box 55, 00014 Helsinki (Finland)
Fax: (+ 358) 9-19150357
E-mail: kristiina.wahala@helsinki.fi

[⁺] Part of this study is included in a PhD thesis by A. Lilienkamp, University of Helsinki, 2007.

ing nonsteroidal structures as 17β -HSD1 inhibitors. These compounds include phytoestrogens,^[25] substituted 2-benzyltetra-1-ones,^[26] benzopyranones,^[27] and phenyl ketones.^[28] In general these nonsteroidal inhibitors have moderate to very low affinity for the enzyme and/or they lack sufficient selectivity. Recently, we have reported a series of compounds based on fused cycloalkenothieno[2,3-*d*]pyrimidin-4(3*H*)-ones to be potent and selective 17β -HSD1 inhibitors.^[29] Also, subsequent to our findings, a series of benzothieno[2,3-*d*]pyrimidin-4(3*H*)-ones has been reported to inhibit 17β -HSD1.^[30]

Although the number of patents and publications concerning 17β -HSD1 inhibition has increased during recent years, surprisingly few studies have included data on QSAR of 17β -HSD1 inhibitors.^[19,20] Potter and co-workers have developed a series of E1 derivatives as 17β -HSD1 inhibitors, where the core of E1 was extended with a substituted pyrazole ring fused to C16 and C17 of ring D of the steroid skeleton.^[20] The binding mode of the two most potent pyrazole derivatives was studied by docking them into the active site of 17β -HSD1 (PDB entry code 1FDT^[8a]), producing superimposition of the steroid nucleus compared with E2 in the crystal structure. The substituents at ring E formed additional hydrogen bond interactions to the cofactor nicotinamide group. A comparative molecular field analysis (CoMFA) model was generated and validated with a small set of compounds. Visual inspection of the correlation between actual and predicted pIC_{50} values showed large variation. In a subsequent study, further modifications of the steroid core and/or pyrazole ring E of the above mentioned skeleton produced a new set of 17β -HSD1 inhibitors.^[19] The inhibitors from these two studies,^[19,20] were used in building a comparative molecular similarity indices analysis (CoMSIA) model. The model was validated with an external set of compounds. A visual inspection of the correlation between the actual and predicted activities showed improvement relative to the earlier study.^[20] All these inhibitors are designed to fit the natural substrate binding pocket and to interact with the catalytic triad residues.

In addition to the human enzyme, a QSAR study of 17β -HSD from the fungus *Cochliobolus lunatus* (17β -HSDcl) has been reported.^[31] 17β -HSDcl has been suggested to be a model enzyme for the short-chain dehydrogenase (SDR) superfamily.^[32] The inhibition activity of variously substituted phytoestrogens (e.g. flavonoids and cinnamic acid esters) was found to be similar between the 17β -HSDcl and human 17β -HSD1 enzymes. The docking studies performed with the flavonoid kaempferol for 17β -HSDcl and human 17β -HSD1, however, suggested different binding modes for this compound.

Structure-based pharmacophore generation has been used as another method to search for new active inhibitors of 17β -HSD1.^[33] Phytoestrogens, known to have moderate inhibitory activity,^[25a,b] were docked into the crystal structure of 17β -HSD1 (PDB entry code 1FDT^[8a]). The results revealed possible hydrogen bonding interaction counterparts in the active site. Using the docking results and the native crystal structure, several pharmacophores were generated and databases screened. As a result, some new inhibitors were suggested.

Herein we report the plausible binding modes and a 3D QSAR model of 17β -HSD1 inhibitors based on a (di)cycloalkenothieno[2,3-*d*]pyrimidin-4(3*H*)-one core and synthesised by our research group.^[29] The binding modes of selected inhibitors have been previously studied using docking,^[18–21] but this is the first study to combine molecular dynamics simulation, docking and 3D QSAR. Because there is evidence that the active site of the aldo-keto reductase enzymes can adapt to the substrate/ligand bound to it and that the cofactor binds prior to the substrate,^[34] we used molecular dynamics simulation (MDS) and docking with the enzyme structure containing the cofactor NADP⁺ (1FDT).^[8a] To relieve the possible unpropitious crystal structure packing effects, and to validate the following MDS procedure, the crystal structure of the 17β -HSD1 enzyme was relaxed with molecular dynamics simulation (see Computational Methods below). The resulting structure was used to dock two potent inhibitors **3** and **4** (Figure 2) into the active site of the enzyme and further MDS

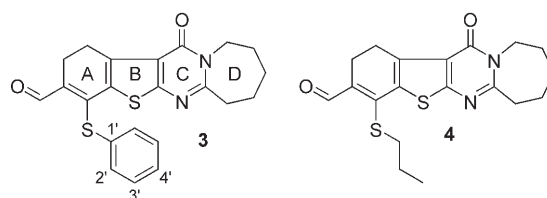


Figure 2. The two potent 17β -HSD1 inhibitors used in the MDS studies and the labelling of the fused ring system.

were performed with these enzyme-cofactor-inhibitor complexes. The active site structure obtained from the MDS with inhibitor **3** was used to dock a molecule library based on a thieno[2,3-*d*]pyrimidin-4(3*H*)-one core into the active site of the enzyme. The binding modes of the inhibitors were studied and a predictive CoMFA model was built using the inhibitor alignment and inhibition data measured in the assay with recombinant human enzyme, rec 17β -HSD1 (Table 1). The model will be used to guide structural modifications of 17β -HSD1 inhibitors based on a thieno[2,3-*d*]pyrimidin-4(3*H*)-one core in order to improve the biological activity as well as in designing novel 17β -HSD1 inhibitors.

Results and Discussion

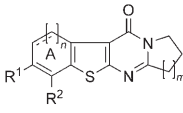
Relaxed structure of the 17β -HSD1–NADP⁺–E2 complex

The crystal structure of 17β -HSD1 complexed with the cofactor NADP⁺ and E2 was relaxed by minimisation and molecular dynamics simulation. After minimisation, an equilibration simulation was performed with restrained backbone, cofactor and E2. During the equilibration, the side chain root mean square deviation (rmsd) was stabilised and the potential energy of the system was stable after an initial increase. Subsequently, an unrestrained simulation for 5 ns was performed. The system stabilised after 2.5 ns showing a relatively constant backbone rmsd curve (Figure 3). The position of E2 was also stabilised after a

Table 1. Structures, biological activities, and pIC₅₀ values of 17 β -HSD1 inhibitors based on the thieno[2,3-*d*]pyrimidin-4(3*H*)-one core.

Compd	R ¹	R ²	Ring A	<i>n</i>	<i>m</i>	rec17 β -HSD1 Inhibition [%] ^[29]		LOGIT ^[a]	pIC ₅₀ Predicted ^[b]
						0.1 μ M	1 μ M		
Training Set									
5			aliphatic	1	3	94.2	96.5	7.83	7.88
6			aliphatic	1	3	87.4	91.9	7.45	7.38
7			aliphatic	1	3	85.6	91.3	7.40	7.34
8			aliphatic	1	3	71.3	94.5	7.32	7.22
9			aliphatic	1	3	67.6	93.4	7.24	7.23
10			aromatic	1	3	80.5	87.5	7.23	7.14
11			aliphatic	1	3	79.2	87.2	7.21	7.16
12			aliphatic	1	3	64.7	92.9	7.19	7.27
4			aliphatic	1	3	58.0	92.4	7.11	7.18
13			aliphatic	1	3	58.5	91.8	7.10	7.07
14			aromatic	1	3	69.0	85.9	7.07	6.98
3			aliphatic	1	3	63.3	85.1	7.00	7.05
15			aliphatic	1	3	46.6	87.4	6.89	7.07
16			aliphatic	1	3	57.4	79.8	6.86	6.93
17			aliphatic	2	3	63.3	74.7	6.85	6.81
18			aliphatic	2	3	38.0	88.1	6.83	6.78
19			aliphatic	1	3	47.0	80.6	6.78	6.83
20			aromatic	1	3	26.9	88.4	6.72	6.84
21			aliphatic	1	3	55.2	64.0	6.67	6.63
22			aliphatic	1	1	16.7	67.2	6.31	6.34
23						24.3	55.8	6.30	6.25
24			aliphatic	1	3	15.3	58.3	6.20	6.25
25			aliphatic	1	3	7.2	30.7	5.77	5.74
26			aliphatic	1	3	4.0	7.8	5.27	5.28
27			aliphatic	1	3	1.1	13.9	5.13	5.08
28						0.0	4.3	4.33	4.34
29			aliphatic	1	1	0.1	2.9	4.27	4.31

Table 1. (Continued)

Compd	R ¹	R ²	Ring A	n	m	rec17β-HSD1 Inhibition [%] ^[29]		LOGIT ^[a]	pIC ₅₀ Predicted ^[b]
						0.1 μM	1 μM		
									
Test Set									
30			aromatic	1	3	83.0	90.6	7.34	7.00
31			aliphatic	1	3	73.4	93.0	7.28	6.93
32			aliphatic	1	3	61.7	92.2	7.14	6.91
33			aliphatic	1	3	51.2	82.2	6.84	6.52
34			aliphatic	1	3	3.8	22.1	6.33	6.52
35			aliphatic	1	3	1.0	16.4	5.95	6.04

[a] pIC₅₀ values acquired from LOGIT transformation. [b] pIC₅₀ values predicted based on the generated CoMFA model.

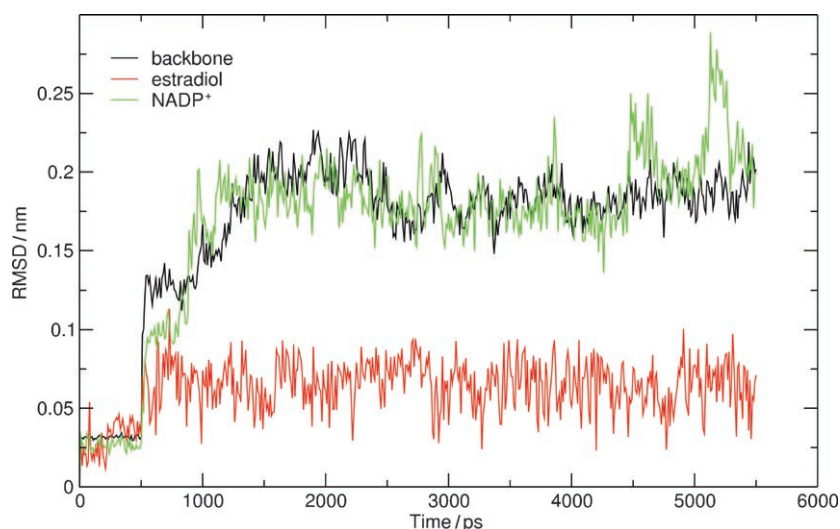


Figure 3. The relaxation of the crystal structure of the 17β-HSD1-NADP⁺-E2 complex (PDB entry code 1FDT). The rmsd of the enzyme backbone is coloured black, the reduced substrate E2 is coloured red, and the cofactor NADP⁺ is coloured green. The first 0.5 ns represents the equilibration simulation with restrained backbone, cofactor, and substrate.

small movement away from NADP⁺ due to the relocation of Phe 192 in the loop at residues 190–200. The rmsd of NADP⁺ was stable from 1 ns onwards but showed a small peak at ~4.5 ns and ~5.1 ns caused by the movement of the ribose ring of the adenosine monophosphate moiety. This part of the cofactor is not located near the active site. In the crystal structure, the distance from the oxidised carbon in NADP⁺ to C17 of E2 is 3.62 Å, while the average of the corresponding distance in the stabilised trajectory was 5.8 Å (Figure 4). This increase in distance may be due to the rejection of the reduced substrate E2 by the enzyme. The backbone of the loop at residues 190–200 kept its initial position during the dynamics and was not flexible as might have been expected due to the vari-

ous conformations observed in the crystal structures. The potential and total energies of the system stabilised at the beginning and remained stable during the whole unrestrained simulation.

In the stable part of the trajectory, there are on average 214 hydrogen bonds within the enzyme and 15 hydrogen bonds between the cofactor and the enzyme. Only an occasional hydrogen bond between E2 and the enzyme was observed. This lack of hydrogen bonding, together with the movement of the substrate, indicates the rejection of the substrate by the enzyme, as can be expected. The rmsd for the active site heavy atoms (residues in a 6 Å sphere around E2) was 2.17 Å between the crystal structure and the relaxed structure. Additionally, the active site cavity volume decreased during the dynamics from ~400 to ~300 Å³, calculated for the united atom structures with the Binding Site Tool in Discovery Studio 1.7.^[35] The rather large rmsd value for the active site atoms, and the decrease in volume indicate conformational changes for active site residues. This emphasises the necessity to properly relax the crystal structures before further studies. The root mean square fluctuation (rmsf), showing the movement of single residues during the MDS, revealed the loop areas and the N and C termini to be the most flexible parts of the enzyme during the simulation. Next, the stabilised trajectory was clustered and

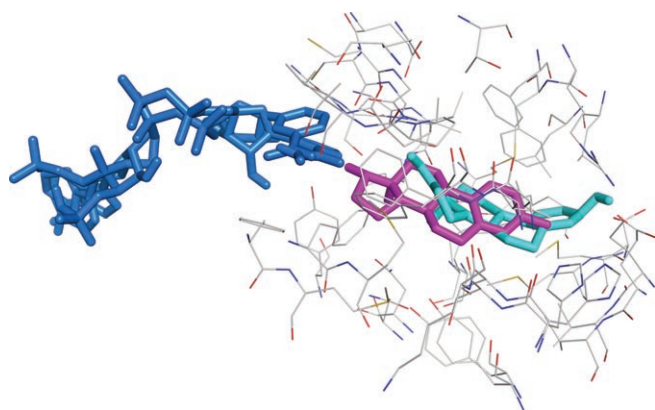


Figure 4. The position of E2 before (magenta) and after (cyan) relaxation. The NADP⁺ cofactor is coloured blue, and the active site residues are represented as thin sticks for clarity.

the representative structure (Figure 4) of the biggest cluster was extracted and minimised in vacuo. In order to acquire an all-atom structure for the subsequent docking of the inhibitors **3** and **4**, the complex was transferred to Insight II,^[36] where E2 was extracted from the active site. Hydrogens were added and the complex was minimised with fixed heavy atoms for 500 steps using the steepest descent algorithm. The resulting cofactor–enzyme complex was used as the enzyme structure for docking the inhibitors.

Generation of the initial 17 β -HSD1–inhibitor complexes

To acquire reasonable starting structures for the MDS, compounds **3** and **4** (Figure 2) were docked into the relaxed structure of the 17 β -HSD1 enzyme using GOLD.^[37] As a result, the inhibitors **3** and **4** were not superimposed, although they share the same fused tetracyclic skeleton. The inhibitors lie in the same plane as E2, but the molecular skeleton of inhibitor **4** is flipped 180 degrees along the long axis of the molecule so, that the thiophene sulfurs and the thioether groups of inhibitors **3** and **4** point in opposite directions. The thiophenyl group and ring A of **3** are nearly superimposed with rings D and B of E2, respectively. With **4**, the skeletal thiophene is nearly superimposed with ring A of E2, and the two terminal carbons of the thiopropyl group are superimposed with C15 and C16 of E2. Compound **3** forms a hydrogen bond from the aldehyde carbonyl to the phenolic hydroxy group of Tyr218, while **4** does not have such an interaction in this binding mode. In addition, compound **3** is orient-

ed to have possible π - π interactions between the thiophene ring and Phe259 and between the aromatic thioether substituent and Phe192. Compound **4** probably has π - π interaction only with Phe259 due to the lack of a thiophenyl side chain. Despite the different orientation of the molecular core, the aldehyde carbonyl and the bulky seven-membered ring D occupy the same space with both **3** and **4**. These inhibitor orientations and interactions with the active site of the enzyme provided rational starting structures for the following MDS studies.

Molecular dynamics simulations of the enzyme complex with inhibitor **3**

The docking of an inhibitor is limited by the rigid or semi-rigid residues of the active site and the binding of an inhibitor is a dynamic rather than static process. In order to find the optimal interactions between the active site and the nonsteroidal inhibitor during the binding, we performed MDS for the 17 β -HSD1–NADP⁺–inhibitor complexes. As was done with the crystal structure of the enzyme complex (see above), an equilibration simulation followed by an unrestrained simulation was performed (see Computational Methods below). The equilibration produced stable side chain rmsd and potential energy curves. In the following unrestrained simulation the system stabilised after 2 ns, showing a stable rmsd curve for the backbone and the inhibitor (Figure 5). The cofactor rmsd increased drastically at ~2.7 ns but returned closer to the starting conformation at ~4.8 ns. This fluctuation was due to the relocation of the cofactor adenosine monophosphate moiety and did not affect the active site geometry. In the beginning of the unrestrained simulation, inhibitor **3** moves away from the cofactor and forms a hydrogen bond from the aldehyde carbonyl to the hydroxy group of Ser222, which is kept for 2 ns. Subsequently, the original position of **3** and the initial hydrogen bond to the phenolic hydroxy group of Tyr218 were restored

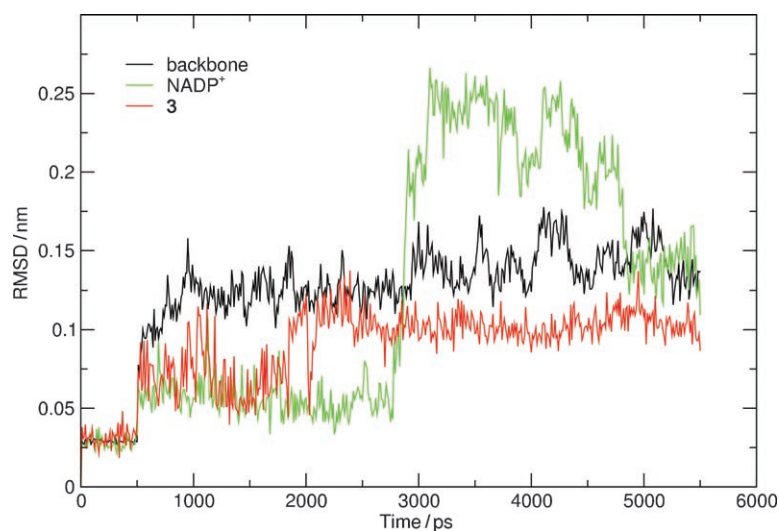


Figure 5. The MDS of the 17 β -HSD1–NADP⁺–**3** complex. The rmsd of the enzyme backbone is coloured black, the inhibitor **3** is coloured red, and the NADP⁺ cofactor is coloured green. The first 0.5 ns represents the equilibration simulation with restrained backbone, cofactor, and inhibitor.

and kept for the rest of the simulation. The aldehyde carbonyl is also involved in hydrogen bond with Asn152. The pyrimidone carbonyl at ring C forms a hydrogen bond to the imidazole group of His221 or the guanidinium group of Arg258. During the MDS, the active site cavity volume did not change significantly relative to the relaxed crystal structure. This indicates that the inhibitor is well tolerated in the active site. The parts of the enzyme that moved the most in MDS (root mean square fluctuation more than 0.1 nm) were the loop areas, as expected. Additionally, the C terminus of the G' helix, the G'' helix located next to the loop area (residues 190–200) and the whole H' and H helices (secondary structure naming from Breton et al.^[6a]) showed movement larger than 0.1 nm, indicating the adaptation of the active site to the inhibitor.

During the stable part of the trajectory (2–5.5 ns), there are on average 218 hydrogen bonds per timeframe within the enzyme, 15 hydrogen bonds between the cofactor and the enzyme and 1.3 hydrogen bonds between inhibitor **3** and the enzyme. In this part of the trajectory, the most stable hydrogen bond between **3** and the enzyme is between the phenolic hydroxy group of Tyr218 to the aldehyde carbonyl oxygen. The active site residues in immediate contact (within 4 Å) with inhibitor **3** during the stable trajectory include Leu96, Ser142, Val143, Gly144, Leu149, Asn152, Gly186, Pro187, Phe192, Met193, Tyr218, His221, Ser222, Arg258, Phe259, Leu262, Met265, Ala278, Met279, Gly282, and Val283. As with the relaxation of the crystal structure, the loop area at residues 190–200 was stable during the simulation.

With a view to obtain a rational enzyme structure for the docking of the molecular library, the stable part of the trajectory was clustered. The representative structure of the biggest cluster was extracted and minimised in vacuo. In this representative structure, the above mentioned hydrogen bonds from inhibitor **3** to Tyr218 and Arg258 were present (Figure 6). The distance from the oxidised carbon in the cofactor to the nearest heavy atom of the inhibitor was 3.8 Å, while in the crystal

structure it was 3.21 Å (from the oxidised carbon in NADP⁺ to the oxygen at C17 of E2). A hydrophobic pocket, formed by residues Val143, Gly144, Leu149, Phe192, Met193 and Phe259, near the catalytic triad accommodates the flexible thiophenyl side chain. The active site (residues 6 Å around the reduced substrate) heavy atom rmsd between the relaxed crystal structure and the representative frame of the enzyme–inhibitor complex trajectory was 1.68 Å, which is less than the value observed in the relaxation of the crystal structure. This suggests minor but still important movement of the active site residues during the inhibitor binding.

The stable volume of the active site, the hydrogen bonding pattern, the nearest heavy atom distance to the cofactor, and the low rmsd value of the active site heavy atoms show that a nonsteroidal inhibitor with a flexible side chain can bind to the active site of 17β-HSD1. Inhibitor **3** does not cause major conformational changes in the enzyme. It was also observed, that the catalytic residues are not involved in the binding.

Molecular dynamics simulations of the enzyme complex with inhibitor **4**

As above with inhibitor **3**, an equilibration simulation followed by an unrestrained simulation was performed for the 17β-HSD1 enzyme complex with inhibitor **4**. The equilibration produced stable side chain rmsd. In the following unrestrained simulation, the stabilisation of the enzyme backbone rmsd with **4** required longer simulation time than the complex with **3** (Figure 7). Owing to the increase in backbone rmsd at the end of the 5 ns simulation (total time 5.5 ns), the system was simulated for an additional 3 ns. The cofactor rmsd had a small drop at ~8.2 ns due to rotation of the terminal phosphate group. Stable backbone, cofactor and inhibitor rmsd were achieved after 5.5 ns.

In the beginning of the unrestrained simulation and also at ~3 ns, an increase in the rmsd of **4** was observed. This increase indicates that the position of **4** was less stable than that of **3**. The inhibitor skeleton was rotated 90 degrees along the long axis of the molecule. This rotation was not observed in the simulation with inhibitor **3**. The stable part of the trajectory has an average of 216 hydrogen bonds within the enzyme, 16 hydrogen bonds between the cofactor and the enzyme and one hydrogen bond between **4** and the enzyme. As with **3**, the MDS showed that a relatively stable hydrogen bond is formed between the aldehyde oxygen of the inhibitor **4** and Tyr218. The aldehyde group is also involved in hydrogen bonding with the amide side chain of

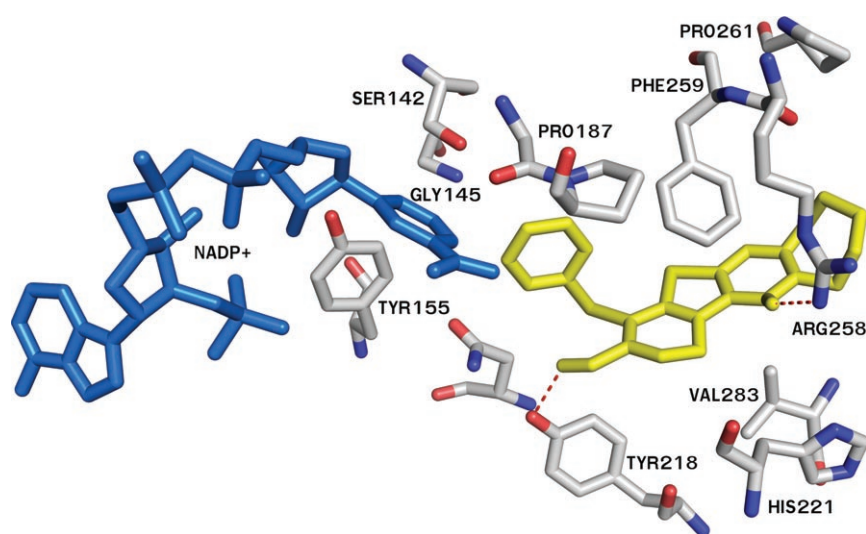


Figure 6. The minimised representative structure of the trajectory with 17β-HSD1, the NADP⁺ cofactor, and inhibitor **3**. The inhibitor is coloured yellow, NADP⁺ is coloured blue, and the hydrogen bonds are indicated as red dashed lines. For clarity, only selected active site residues are displayed.

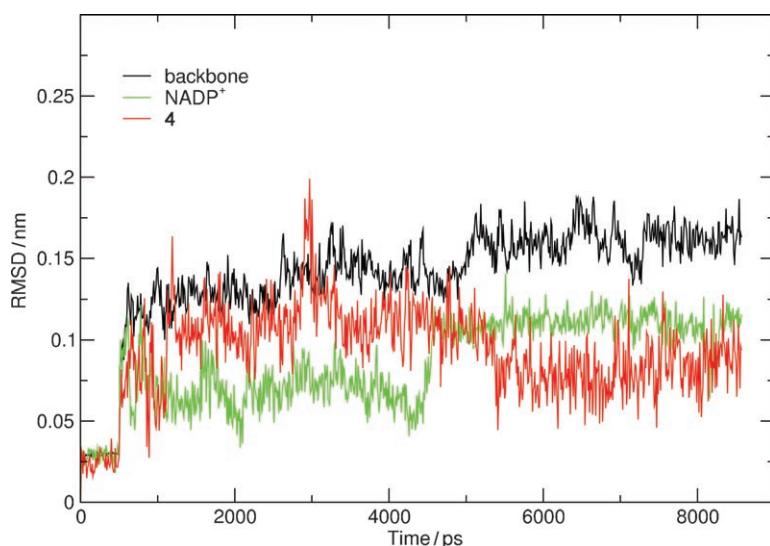


Figure 7. The MDS of the 17 β -HSD1–NADP⁺–4 complex. The rmsd of the backbone of the enzyme is coloured black, the inhibitor 4 is coloured red, and the NADP⁺ cofactor is coloured green. The first 0.5 ns represents the equilibration simulation with restrained backbone, cofactor, and inhibitor.

Asn152. The pyrimidone imine nitrogen of the inhibitor formed an occasional hydrogen bond to the imidazole group of His221. The rmsf showed that secondary structures of the enzyme showing largest movements were the C terminus of the G' helix and the G'' helix. In general, the MDS with inhibitors were more stable than the relaxation of the crystal structure, probably due to the release of the packing effects during the crystallisation. The active site residues in immediate contact (within 4 Å) with the inhibitor 4 during the stable part of the trajectory include Gly144, Met147, Leu149, Phe192, Met193, Tyr218, His221, Ser222, Val225, Phe226, Arg258, Phe259, Pro261, Leu262, Met279, Gly282 and Val283. The loop area at residues 190–200 remained stable during the dynamics.

The trajectory from 5.5 to 8 ns was clustered and the representative structure of the biggest cluster was extracted and minimised in vacuo (Figure 8). The hydrogen bond from the aldehyde group in 4 to Tyr218 was present. Arg258, which formed a hydrogen bond with inhibitor 3, is in this complex turned away from inhibitor 4 and interacts with the solvent instead. Similarly, His221 does not interact with the inhibitor, as it did with inhibitor 3, but forms a stable hydrogen bond with Glu282. The distance from the oxidised carbon of the cofactor to the nearest heavy atom of the inhibitor 4 is 7.04 Å. This is significantly larger

than corresponding distances of the relaxed crystal structure (4.46 Å) or the simulated complex with inhibitor 3 (3.8 Å). The active site heavy atom rmsd between the relaxed crystal structure and the representative frame of the 17 β -HSD1–4 complex trajectory was clearly larger than with inhibitor 3, namely 2.16 Å. Additionally, the active site cavity volume decreased from ~300 Å³ (relaxed structure) to ~250 Å³ (representative frame of the 17 β -HSD1–4 complex trajectory) causing inhibitor 4 to protrude partially out of the active site. It is notable that the catalytic residues (Ser142, Tyr155 and Lys159) are located too far to interact with either of the inhibitors 3 or 4.

Together these facts (the increase in distance to the cofactor, the rotation of the inhibitor during the dynamics, the larger active site heavy atom rmsd and the decrease in active site cavity volume) indicate a less stable behaviour of inhibitor 4 in the active site. Therefore, it can be concluded that the initial position of inhibitor 4 in the active site was less favoured relative to inhibitor 3 in the MDS.

The binding mode of 17 β -HSD1 inhibitors based on the thieno[2,3-*d*]pyrimidin-4(3*H*)-one core

The representative frame of the 17 β -HSD1–3 complex trajectory was selected for the docking studies due to the more stable

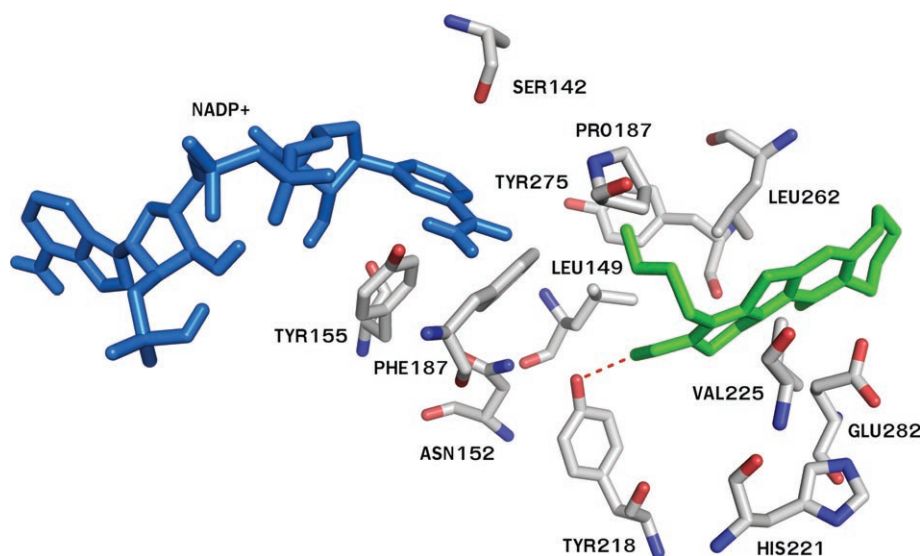


Figure 8. The minimised representative structure of the trajectory with 17 β -HSD1, the NADP⁺ cofactor, and inhibitor 4. The inhibitor is coloured green, NADP⁺ is coloured blue, and the hydrogen bonds are indicated as red dashed lines. For clarity, only selected active site residues are displayed.

behaviour of inhibitor **3** during the MDS. A set of synthesised thieno[2,3-*d*]pyrimidin-4(3*H*)-one based inhibitors **3–35** (Table 1),^[29] were docked into the active site of the 17 β -HSD1 enzyme to investigate the binding modes of the compounds. As a result of the docking, the orientation of inhibitor **3** from the MDS was reproduced. The trend of the scores of the inhibitors **3–35**, excluding some outliers, followed the reported biological activity. In the top-ranked pose of each inhibitor there is a hydrogen bond from ring A aldehyde or hydroxy group to Tyr218 and/or Asn 152, and from the amide carbonyl at ring C to Arg258. The same hydrogen bond interactions were observed for inhibitor **3** during the MDS. The hydrophobic pocket, revealed in the MDS with inhibitor **3**, contributes to the binding accommodating the flexible thioether side chain of the inhibitors. The pocket is formed by residues Val143, Gly144, Leu149, Phe192, Met193 and Phe259. The best inhibitor in the series is compound **5**, which had the above mentioned interactions, and an additional hydrogen bond from the phenolic hydroxy group at C3' of thiophenyl moiety to the backbone carbonyl of Gly144 (Figure 9). A comparison between the product E2 and the most potent inhibitor **5** shows completely different interactions in the active site of the enzyme (Figure 10).

The other potent inhibitors contain a thiophenyl group in ring A with a small C2' or C4' hydroxy group, or a C4' fluorine substituent (compounds **7**, **13** and **6**). Compounds with an aromatic ring A are also active (compounds **10**, **14** and **30**). Compound **11** with a C4' pyridylthio substituent seems to bind with a relatively high affinity, although according to docking, the active site lacks a suitable hydrogen bonding counterpart for the pyridyl nitrogen. The less potent inhibitors have either a bulky C4' tolyl, naphthyl, benzyl or a morpholinolyl thioether side chain (compounds **19**, **21**, **25**, **26**). Inhibitors with a smaller than seven-membered or absent ring D (compounds **22**, **23**, **28** and **29**) also result in relatively weak inhibition. A carboxyl or an amino substituent in the thiophenyl moiety, as in compounds **34** and **35**, seem not to be tolerated. Larger D-rings seem to be favoured, although the bulky ring partially pro-

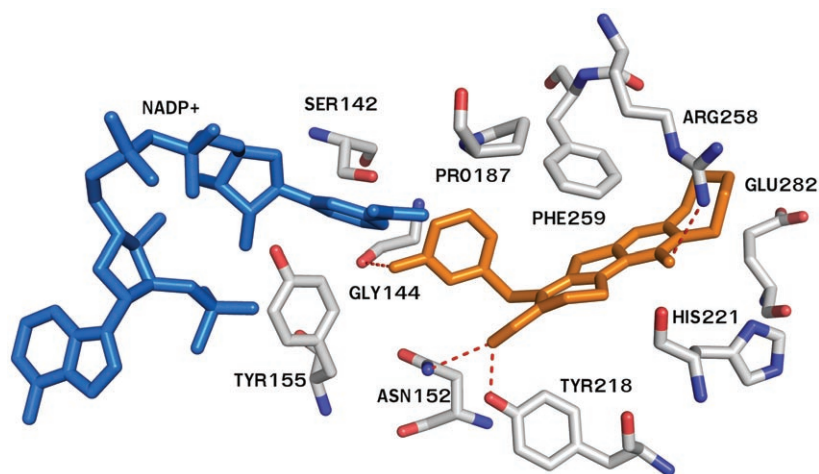


Figure 9. The most potent inhibitor **5** (orange) in the active site of 17 β -HSD1. The NADP⁺ cofactor is coloured blue, and the hydrogen bonds are indicated as red dashed lines. For clarity, only selected active site residues are displayed.

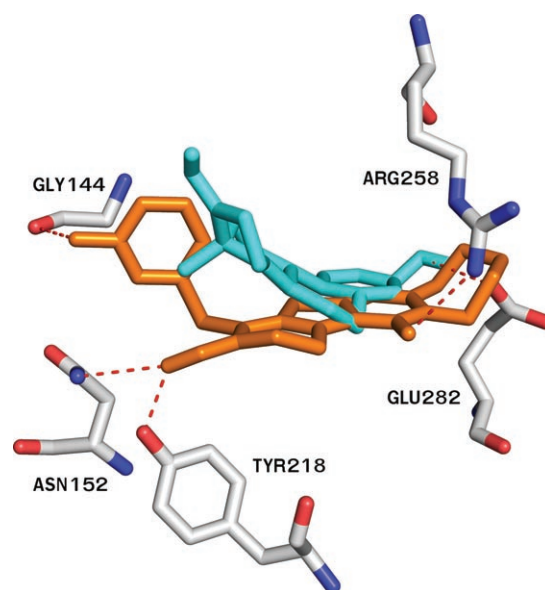


Figure 10. The natural product E2 (cyan) and the most potent inhibitor **5** (orange) in the active site of the enzyme. Only the interacting residues are displayed for clarity.

trudes from the active site to the surface of the enzyme. The positive effect is probably due to a quite hydrophobic active site cavity opening formed by Val225, Phe259, Leu262, Met265 and Ala278. The only non-hydrophobic residue in the opening is Glu282.

The inhibitory activity of compounds **3–35** was in good correlation with the ranking obtained from the dockings. In addition, the inhibitors were very well superimposed. Docking of compounds with an unsubstituted ring A resulted in a different binding mode, in which the fused tetracyclic skeleton is flipped horizontally and/or vertically relative to the inhibitors used in the MDS study (data not shown). These unsubstituted compounds are not biologically active and were omitted from the CoMFA model building.

The CoMFA model of 17 β -HSD1 inhibitors

A 3D QSAR model using the CoMFA method was built in order to quantify the contributions of variable functional groups to the biological activity of the inhibitors based on a thieno[2,3-*d*]pyrimidin-4(3*H*)-one core. The good alignment (Figure 11) of the 17 β -HSD1 inhibitors and the correlation between ranking and biological activity encouraged us to build a 3D QSAR model using the CoMFA method. Charges were assigned and CoMFA descriptors were generated. The LOGIT

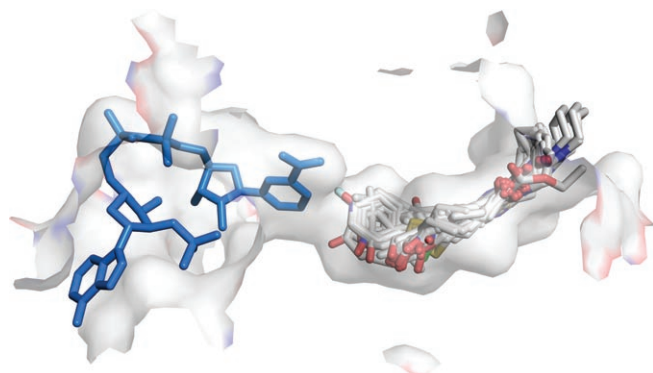


Figure 11. The alignment of inhibitors 3–29 acquired by docking the library to the representative structure of the enzyme–cofactor–inhibitor 3 trajectory. The NADP⁺ cofactor is coloured blue, and the active site is displayed as a transparent surface.

transformed pIC_{50} values (Table 1) were used as dependant variables and a PLS regression analysis was performed with a leave-one-out (LOO) internal cross-validation procedure. A q^2_{LOO} value of 0.602, with standard error of prediction (SEP) value of 0.640, was obtained confirming the predictive power of the model. A more robust cross-validation was done with five random groups yielding a q^2_5 value of 0.601 and a SEP value of 0.641, further validating the model. Four compounds were identified as outliers and were omitted from the final model and a training set of 27 compounds was used (Table 1). A non-cross-validated PLS analysis with five components was performed giving a correlation (r^2) value of 0.994 between the LOGIT transformed and the predicted activities, with a standard error of estimate (SEE) of 0.077. The steric and electrostatic contributions to the final model were 45% and 55%, respectively. The final validation of the QSAR model was done with an external test set, that is, predicting the activities of compounds not used in generating the model. The activities of six compounds (Table 1, Test set) were predicted using the generated CoMFA model. The LOGIT transformed and predicted pIC_{50} values are listed in Table 1 and their correlation in Figure 12. The predicted biological activities are in good agreement with the linear correlation line obtained from the training set, which confirms that the model can be used in estimating the activities of inhibitors sharing a similar molecular skeleton and binding mode. The biological activities of the compounds in the test set were predicted within 0.4 units from their LOGIT transformed pIC_{50} values. A visual inspection of the CoMFA fields (StdDev*Coeff field type) shows areas where the steric and electrostatic interactions are favoured or disfavoured. In Figure 13a, the areas where the steric interactions are favoured (green, 80% of the overall range of values) and disfavoured (yellow, 20% of the overall range of values) are presented together with the most active inhibitor 5. In Figure 13b, the areas where a positive charge is favoured (blue, 80%) and disfavoured (red, 20%) are presented together with the most active inhibitor 5. The largest area favouring steric interactions is located near the bulky thiophenyl moiety. This indicates that a suitable substituent at C3' and/or C2' positions of the thiophenyl ring would enhance binding to the 17 β -HSD1 enzyme.

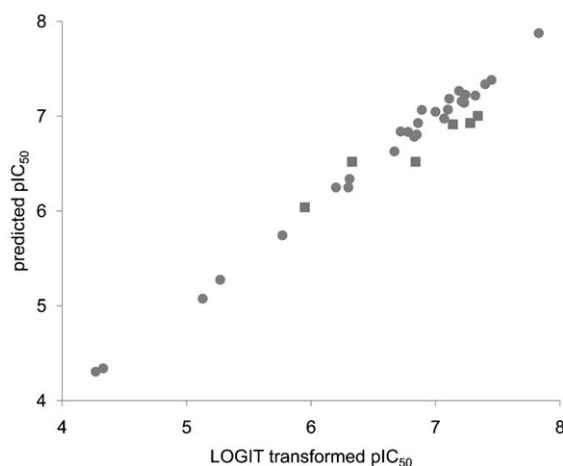


Figure 12. The correlation between the LOGIT transformed and predicted pIC_{50} values obtained from the CoMFA model based on a training set of 27 compounds (●) and a test set of six compounds (■).

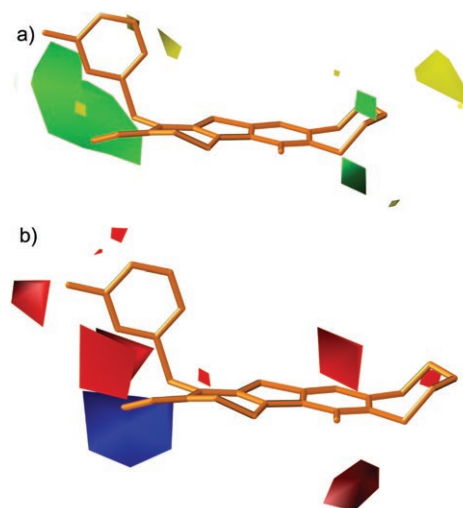


Figure 13. a) The CoMFA fields showing the areas where steric interactions are favoured (green) and unfavoured (yellow); the most potent inhibitor 5 is displayed in orange. b) The CoMFA fields showing the areas where positive charge is favoured (blue) and negative charge is favoured (red); the most potent inhibitor 5 is displayed in orange.

It should be noted that a thionaphthyl substituent is too large in this position, as can be observed in comparing the activities of compounds 3 and 21 (Table 1).

A relatively large blue area, showing the favourable effect of a positive charge, is located next to the aldehyde carbonyl group, indicating that a more positive charge would enhance the inhibitory activity. This can be seen by comparing compounds 10, 31, and 3, for which a hydroxy group results in better inhibition than an aldehyde group. If the CoMFA fields are superimposed on the inhibitor 3–enzyme complex, the largest sterically favoured area is accommodated by the hydrophobic pocket in the active site. The area where a positive charge is favoured (blue) is located near the phenolic hydroxy group of Tyr218. It should be noted, however, that most of the compounds with an aldehyde group are already potent inhibi-

tors and a hydroxy group at the same position produces better inhibition. Areas suggesting less positive charge (red) are located near the side chain amide group of Asn 152 and Arg 258. Suitable functional groups at these locations could provide hydrogen bonding counterparts for these active site residues. The CoMFA fields, especially combined with the 3D-structure of the active site, can guide the structural modifications of 17 β -HSD1 inhibitors based on the thieno[2,3-*d*]pyrimidin-4(3*H*)-one core.

Conclusions

We have investigated the binding modes of selected 17 β -HSD1 inhibitors based on thieno[2,3-*d*]pyrimidin-4(3*H*)-ones combining molecular dynamics simulation, ligand-protein docking, and 3D QSAR. This is the first time these methods have been combined to identify important active site residues and to quantify structural features related to nonsteroidal inhibitors of 17 β -HSD1. The MDS with a potent inhibitor **3** showed stable behaviour of the enzyme-inhibitor complex and revealed that the active site can bind compounds which are not as planar as estrogens. It was found, that flexible and bulky inhibitor side chains can be accommodated by a hydrophobic pocket located near the C terminus of β strand E. The catalytically active residues Ser 142, Tyr 155 and Lys 159, which have been suggested to interact with steroidal inhibitors, were shown not to be required for binding of these nonsteroidal inhibitors. A docking study, which used the active site geometry from the MDS with a potent inhibitor **3**, revealed that residues Tyr 218, Asn 152, Arg 258 and His 221 act as hydrogen bonding counterparts for the thieno[2,3-*d*]pyrimidin-4(3*H*)-one based inhibitors. The inhibitory activity of the most potent compound **5** could be explained by an additional hydrogen bond formed between the side chain phenolic hydroxy group and backbone carbonyl of Gly 144.

A 3D QSAR model employing the CoMFA method was generated using inhibition data from the rec17 β -HSD1-based assay and the alignment of the inhibitor library from the docking. The model was built with the most extensive training set to date and was validated with an external test set. The predicted activities of the test set were in good agreement with the experimentally tested values. The active site structures obtained from the MDS along with the generated 3D QSAR model provide valuable guidelines for further development of 17 β -HSD1 inhibitors based on the dicycloalkenothieno[2,3-*d*]pyrimidin-4(3*H*)-one core. In addition, the CoMFA model can be employed in design of novel 17 β -HSD1 inhibitors.

Computational Methods

The crystal structure of the 17 β -HSD1-NADP⁺-E2 complex^[8a] (PDB entry code 1FDT) was downloaded from the Protein Data Bank.^[38] Molecular modelling software Insight II^[36] and Gromacs version 3.3.1^[39] were used for protein minimisation and molecular dynamics simulations (MDS). GOLD version 3.1.1^[37] and Surflex-Dock^[40] implemented in Sybyl 7.3 software,^[41] were used for docking studies. A comparative molecular field analysis (CoMFA)^[42] model was

built using the QSAR module implemented in Sybyl 7.3. The calculations were performed on an IBM-compatible desktop workstation, an SGI O₂+ workstation and an HP ProLiant DL145 cluster supercomputer. All small molecules were sketched and minimised in Sybyl 7.3 (Tripos force field) and molecular graphics were generated with PyMOL version 0.99^[43] and Sybyl 7.3. The ligands were prepared with the PRODRG server^[44] and modified to GROMOS96 (ffG43a1) force field in Gromacs.

17 β -HSD1-NADP⁺-E2 complex 1FDT^[8a] was selected for the MDS and dockings due to the presence of both co-crystallised cofactor NADP⁺ and the reduced substrate E2. The crystal structure contains double coordinates (marked as A and B in the PDB file) for residues 192–198 (the flexible loop area) and for a single residue Arg37, located in a loop between β strand B and α helix C, possibly interacting with the cofactor. Relaxation of the crystal structure, that is, minimisation followed by molecular dynamics, was performed with both resolved flexible loop and Arg37 conformations. The conformation where the Arg37 side chain clashes with the cofactor and the loop is in a conformation where Phe192 is exposed to solvent (chain A in the PDB file) produced disturbed behaviour of the cofactor (data not shown). The other alternative (chain B in the PDB file) yielded a stable MDS trajectory and was therefore selected for the in-depth analysis of the MDS and for the inhibitor docking studies.

Relaxation of the crystal structure of the 17 β -HSD1-NADP⁺-E2 complex

The crystal structure was relaxed using Gromacs software in order to remove possible unfavourable effects resulting from crystal packing. Prior to the relaxation of the complex, all water molecules and sulfate ions in the PDB file were deleted. The complex consisting of the enzyme, NADP⁺ (NDPP topology in GROMOS96 ffG43a1 force field containing charged pyridine nitrogen) and E2 was put into a truncated octahedron box of ~8400 water molecules with a total volume of 304 nm³. In order to neutralise the system and to create conditions mimicking physiological saline, a total of 59 water molecules were replaced with 31 Na⁺ and 28 Cl⁻ ions in random order. The neutralised system was minimised to acquire a reasonable starting structure for the MDS. The temperature was set to 310 K and periodic boundary conditions were applied with neighbour list update frequency of 10 steps and a 0.9 nm cut-off for neighbour searching. Long-range electrostatics were treated with particle-mesh Ewald (PME) method and a 1.4 nm cut-off applied to treat van der Waals interactions. The system temperature and pressure were coupled with Berendsen algorithms and hydrogen containing bonds were constrained with the LINCS algorithm.^[45] A 0.5 ns simulation with a time step of 2 fs was performed with restrained (1000 kJ mol⁻¹ nm⁻² restraining force) protein backbone, cofactor and E2 in order to adapt the side chains and water molecules to their surroundings. After the equilibration, the system was simulated unrestrained for 5 ns with the same parameters.

Initial 17 β -HSD1-inhibitor complexes

Two potent 17 β -HSD1 inhibitors **3** and **4** (Figure 2), based on the thieno[2,3-*d*]pyrimidin-4(3*H*)-one core^[29] were selected for the MDS studies. These two inhibitors differ only in the thioether moiety; compound **3** has an aromatic thiophenyl group at the fused ring A, whereas **4** has an aliphatic thiopropyl group at the same position. Inhibitors **3** and **4** were docked into the active site of the relaxed crystal structure containing the cofactor using Gold 3.1.1

software. The default settings were used and the active site was defined as a 10 Å sphere around a side chain hydrogen atom of Leu 149 with cavity detection enabled. The GoldScore scoring function was used to rank the inhibitors. As a result, only one pose for **4** and two very similar poses for **3** were acquired. These enzyme-cofactor-inhibitor complexes were used as starting structures for MDS studies.

Molecular dynamics simulations with inhibitors 3 and 4

The enzyme-cofactor-inhibitor complex was subjected to MDS containing either inhibitor **3** or **4** docked into the active site of the relaxed crystal structure. These complexes were again put into a water box with ~8700 water molecules and 32 Na⁺ and 29 Cl⁻ ions. The complexes were energy minimised and equilibrated with a 0.5 ns simulation with a restrained backbone, cofactor and inhibitor. Subsequently, an unrestrained simulation was performed. The same MDS parameters were used as described above for the relaxation of the crystal structure.

Building the CoMFA model

A training set of 27 compounds (Table 1) was selected using the biological activity measured in the recombinant 17 β -HSD1 assay. The biological data for the inhibitors was reported as an inhibition percentage at two concentrations: 0.1 and 1 μ M.^[29] The IC₅₀ values for the inhibitors were estimated from the inhibition percentages using LOGIT transformation.^[46] The value produced by this transformation is the correction to the p(log) value of the concentration, in this case 6 or 7. These corrections were used to produce the pIC₅₀ values of the inhibitors (Table 1). The docking of the training set was performed with the Surflex-Dock module implemented in Sybyl software. The protocol creation was automated and ring flexibility and pre- and post-dock minimisations were enabled. The inhibitor alignment was achieved using the top-ranked pose for each inhibitor yielding a uniform binding mode and a good superimposition of the functional groups. Gasteiger-Hückel charges were assigned for the inhibitors and CoMFA descriptors were generated using the QSAR module of Sybyl. A leave-one-out cross-validation was performed. In this validation method each of the inhibitors is in turn omitted from the model and the activity of the omitted inhibitor is predicted based on the generated model. Further validation was done with random group validation, creating five random groups. One group at a time is omitted from the model and the activities of the members of the omitted group are predicted based on the generated model. Finally, a partial least squares (PLS) regression analysis was performed using the LOGIT transformed pIC₅₀ values as dependent variables and five components.

Acknowledgements

Prof. Dr. Hans-Dieter Höltje is acknowledged for scientific advice, and Dr. Atte Sillanpää and Ms. Birte Brandt, for technical advice. The Finnish IT Center for Science (CSC) is acknowledged for computer time allocation, and The Academy of Finland is acknowledged for funding (grants 78226, 78253, and 210633).

Keywords: 17 β -HSD1 • 3D QSAR • breast cancer • drug design • molecular modeling

- [1] A. Jemal, R. Siegel, E. Ward, T. Murray, J. Xu, M. J. Thun, *CA Cancer J. Clin.* **2007**, *57*, 43–66.
- [2] a) H. J. Smith, P. J. Nicholls, C. Simons, R. Le Lain, *Expert Opin. Ther. Pat.* **2001**, *11*, 789–824; b) J. R. Pasqualini, *Biochim. Biophys. Acta* **2004**, *1654*, 123–143; c) J. R. Pasqualini, G. S. Chetrite, *J. Steroid Biochem. Mol. Biol.* **2005**, *93*, 221–236; d) W. R. Miller, *Best Pract. Res. Clin. Endocrinol. Metab.* **2004**, *18*, 1–32.
- [3] a) G. Möller, J. Adamski, *Mol. Cell. Endocrinol.* **2006**, *248*, 47–55; b) P. Lukacik, K. L. Kavanagh, U. Opperman, *Mol. Cell. Endocrinol.* **2006**, *248*, 61–71.
- [4] a) Y. Hong, S. Chen, *Ann. N. Y. Acad. Sci.* **2006**, *1089*, 237–251; b) R. W. Brueggemeier, *Expert Opin. Pharmacother.* **2006**, *7*, 1919–1930.
- [5] a) S. Karkola, H.-D. Höltje, K. Wähälä, *J. Steroid Biochem. Mol. Biol.* **2007**, *105*, 63–70; b) A. D. Favia, A. Cavalli, M. Masetti, A. Carotti, M. Recanatini, *Proteins Struct. Funct. Genet.* **2006**, *62*, 1074–1087; c) C. Loge, M. Le Borgne, P. Marchand, J. M. Robert, G. Le Baut, M. Palzer, R. W. Hartmann, *J. Enzyme Inhib. Med. Chem.* **2005**, *20*, 581–585; d) S. Chen, F. Zhang, M. A. Sherman, I. Kijima, M. Cho, Y. C. Yuan, Y. Toma, Y. Osawa, D. Zhou, E. T. Eng, *J. Steroid Biochem. Mol. Biol.* **2003**, *86*, 231–237; e) A. Cavalli, G. Greco, E. Novellino, M. Recanatini, *Bioorg. Med. Chem.* **2000**, *8*, 2771–2780.
- [6] H. Jörnvall, B. Persson, M. Krook, S. Atrian, R. Gonzalez-Duarte, J. Jeffery, D. Ghosh, *Biochemistry* **1995**, *34*, 6003–6013.
- [7] D. Ghosh, V. Z. Pletnev, D.-W. Zhu, Z. Wawrzak, W. L. Duax, W. Panghorn, F. Labrie, S.-X. Lin, *Structure* **1995**, *3*, 503–513.
- [8] a) R. Breton, D. Housset, C. Mazza, J. C. Fontecilla-Camps, *Structure* **1996**, *4*, 905–915; b) A. Azzi, P. H. Rehse, D.-W. Zhu, R. L. Campbell, F. Labrie, S.-X. Lin, *Nat. Struct. Biol.* **1996**, *3*, 665–668; c) M. W. Sawicki, M. Erman, T. Puranen, P. Vihko, D. Ghosh, *Proc. Natl. Acad. Sci. USA* **1999**, *96*, 840–845.
- [9] a) Q. Han, R. L. Campbell, A. Gangloff, Y.-W. Huang, S.-X. Lin, *J. Biol. Chem.* **2000**, *275*, 1105–1111; b) A. Gangloff, R. Shi, V. Nahoum, S.-X. Lin, *FASEB J.* **2003**, *17*, 274–276; c) R. Shi, S.-X. Lin, *J. Biol. Chem.* **2004**, *279*, 16778–16785.
- [10] W. Qiu, R. L. Campbell, A. Gangloff, P. Dupuis, R. P. Boivin, M. R. Tremblay, D. Poirier, S.-X. Lin, *FASEB J.* **2002**, DOI: 10.1096/fj.02-0026fj.
- [11] a) S. Alho-Richmond, A. Lilienkampff, K. Wähälä, *Mol. Cell. Endocrinol.* **2006**, *248*, 208–213; b) “Enhancement of synthetic SPROUT de novo ligand design program knowledge base. SPROUT application for 17 β -hydroxysteroid dehydrogenase type 1 enzyme”: S. Alho, PhD thesis, University of Helsinki, **2005**.
- [12] J. Blanchet, S. X. Lin, B. S. Zhorov, *Biochemistry* **2005**, *44*, 7218–7227.
- [13] a) H. Peltoketo, V. Isomaa, O. Mäentausta, R. Vihko, *FEBS Lett.* **1988**, *239*, 73–77; b) S.-X. Lin, F. Yang, J.-Z. Jin, R. Breton, D.-W. Zhu, V. Luu-The, F. Labrie, *J. Biol. Chem.* **1992**, *267*, 16182–16187.
- [14] C. Gunnarsson, M. Ahnström, K. Kirschner, B. Olsson, B. Nordenskjöld, L. E. Rutqvist, L. Skoog, O. Stål, *Oncogene* **2003**, *22*, 34–40.
- [15] a) M. Poutanen, V. Isomaa, V. Lehto, P. Vihko, *Int. J. Cancer* **1992**, *50*, 386–390; b) M. M. Miettinen, M. H. Poutanen, R. K. Vihko, *Int. J. Cancer* **1996**, *68*, 600–604; c) H. Sasano, A. R. Frost, R. Saitoh, N. Harada, M. Poutanen, R. Vihko, S. E. Bulun, S. G. Silverberg, H. Nagura, *J. Clin. Endocrinol. Metab.* **1996**, *81*, 4042–4046; d) T. Suzuki, T. Moriya, N. Ariga, C. Kaneko, M. Kanazawa, H. Sasano, *Br. J. Cancer* **2000**, *82*, 518–523.
- [16] For a review see a) D. Poirier, *Curr. Med. Chem.* **2003**, *10*, 453–477; b) T. M. Penning, *Endocr. Relat. Cancer* **1996**, *3*, 41–56; c) M. R. Tremblay, D. Poirier, *J. Steroid Biochem. Mol. Biol.* **1998**, *66*, 179–191.
- [17] a) B. Husen, K. Huhtinen, T. Saloniemi, J. Messinger, H. H. Thole, M. Poutanen, *Endocrinology* **2006**, *147*, 5333–5339; b) B. Husen, K. Huhtinen, M. Poutanen, L. Kangas, J. Messinger, H. Thole, *Mol. Cell. Endocrinol.* **2006**, *248*, 109–113.
- [18] H. R. Lawrence, N. Vicker, G. M. Allan, A. Smith, M. F. Mahon, H. J. Tutill, A. Purohit, M. J. Reed, B. V. L. Potter, *J. Med. Chem.* **2005**, *48*, 2759–2762.
- [19] G. M. Allan, H. R. Lawrence, J. Cornet, C. Bubert, D. Fischer, N. Vicker, A. Smith, H. J. Tutill, A. Purohit, J. Day, M. F. Mahon, M. J. Reed, B. V. L. Potter, *J. Med. Chem.* **2006**, *49*, 1325–1345.
- [20] D. S. Fischer, G. M. Allan, C. Bubert, N. Vicker, A. Smith, H. J. Tutill, A. Purohit, L. Wood, G. Packham, M. F. Mahon, M. J. Reed, B. V. L. Potter, *J. Med. Chem.* **2005**, *48*, 5749–5770.
- [21] N. Vicker, H. R. Lawrence, G. M. Allan, C. Bubert, A. Smith, H. J. Tutill, A. Purohit, J. H. Day, M. F. Mahon, M. J. Reed, B. V. L. Potter, *ChemMedChem* **2006**, *1*, 464–481.

- [22] a) "Novel 17 β -hydroxysteroid dehydrogenase type 1 inhibitors": J. Messinger, H.-H. Thole, B. Husen, B. J. Van Steen, G. Schneider, J. B. E. Hulshof, P. Koskimies, N. Johansson, J. Adamski, PCT Int. Appl. WO 2005/047303A2, May 26, **2005**; b) "17 β -HSD1 and STS inhibitors": J. Messinger, H.-H. Thole, B. Husen, P. Koskimies, L. Pirkkala, M. Weske, PCT Int. Appl. WO 2006/125800A1, November 30, **2006**.
- [23] a) "Novel 2-substituted Δ -homoestra-1,3,5(10)-trienes as inhibitors of 17 β -hydroxysteroid dehydrogenase type 1": C. Gege, W. Regenhard, O. Peters, A. Hillisch, J. Adamski, G. Möller, D. Deluca, W. Elger, B. Schneider, PCT Int. Appl. WO2006/003012A1, January 12, **2006**; b) "Novel 2-substituted estra-1,3,5(10)-trien-17-ones used in a form of inhibitors of 17 β -hydroxysteroid dehydrogenase type 1": A. Hillisch, W. Regenhardt, C. Gege, O. Peters, U. Bothe, J. Adamski, G. Möller, A. Rosinius, W. Elger, B. Schneider, PCT Int. Appl. WO2006/003013A2, January 12, **2006**; c) D. Deluca, G. Möller, A. Rosinus, W. Elger, A. Hillisch, J. Adamski, *Mol. Cell. Endocrinol.* **2006**, *248*, 218–224.
- [24] a) D. Poirier, R. P. Boivin, M. Berube, S.-X. Lin, *Synth. Commun.* **2003**, *33*, 3183–3192; b) D. Poirier, R. P. Boivin, M. Tremblay, M. Berube, W. Qiu, S.-X. Lin, *J. Med. Chem.* **2005**, *48*, 8134–8147; c) M. Berube, D. Poirier, *Org. Lett.* **2004**, *6*, 3127–3130.
- [25] a) S. Mäkelä, M. Poutanen, J. Lehtimäki, M.-L. Kostian, R. Santti, R. Vihko, *Proc. Soc. Exp. Biol. Med.* **1995**, *208*, 51–59; b) S. Mäkelä, M. Poutanen, M.-L. Kostian, J. Lehtimäki, L. Strauss, R. Santti, R. Vihko, *Proc. Soc. Exp. Biol. Med.* **1998**, *217*, 310–316; c) J. C. Le Bail, T. Laroche, F. Marre-Fournier, G. Habrioux, *Cancer Lett.* **1998**, *133*, 101–106; d) J. D. Brooks, L. U. Thompson, *J. Steroid Biochem. Mol. Biol.* **2005**, *94*, 461–467; e) D. Deluca, A. Krazeisen, R. Breitling, C. Prehn, G. Möller, J. Adamski, *J. Steroid Biochem. Mol. Biol.* **2005**, *93*, 285–292.
- [26] "Benzyl tetralins, formulations and uses thereof": H. J. Smith, P. Mason, M. Ahmadi, P. J. Nicholls, V. Greer, WO0142181, June 14, **2001**.
- [27] "Tetralone or benzopyranone derivatives and a method for producing them": M. Yoshima, M. Nakakoshi, J. Nakamura, S. Nakayama, US6080781, June 27, **2000**.
- [28] R. K. Lota, S. Dhanani, C. P. Owen, S. Ahmed, *Lett. Drug Des. Discovery* **2007**, *4*, 180–184.
- [29] a) A. Lilienkamp, S. Alho-Richmond, P. Koskimies, N. Johansson, K. Huhtinen, K. Vihko, K. Wähälä, unpublished results; b) "Preparation of fused thiophenopyrimidones as 17 β -hydroxysteroid dehydrogenase inhibitors": K. Wähälä, A. Lilienkamp, S. Alho, K. Huhtinen, N. Johansson, P. Koskimies, K. Vihko, PCT Int. Appl. WO2004110459A1, December 23, **2004**; c) "Therapeutically active thiophenopyrimidone compounds and their use": K. Wähälä, A. Lilienkamp, S. Alho, K. Huhtinen, N. Johansson, P. Koskimies, K. Vihko, U.S. Patent Appl. A120050032778, October 2, **2005**.
- [30] a) "Preparation of benzothienopyrimidinones as inhibitors of 17 β -hydroxysteroid dehydrogenase": L. Hirvelä, N. Johansson, P. Koskimies, O. T. Pentikäinen, T. Nyrönen, T. A. Salminen, M. S. Johnson, P. Lehtovuori, P. Saarenketo, B. J. Van Steen, H.-H. Thole, M. Unkila, J. Messinger, J. Kiviniemi, L. Pirkkala, B. Husen, U.S. Pat. Appl. 2005176742A1, November 8, **2005**; b) J. Messinger, L. Hirvelä, B. Husen, P. Koskimies, O. Pentikäinen, P. Saarenketo, H.-H. Thole, *Mol. Cell. Endocrinol.* **2006**, *248*, 192–198.
- [31] M. Sova, A. Perdih, M. Kotnik, K. Kristan, T. Lanisnik Rizner, T. Solmajerb, S. Gobeca, *Bioorg. Med. Chem.* **2006**, *14*, 7404–7418.
- [32] K. Kristan, K. Krajnc, J. Konc, S. Gobec, J. Stojan, T. Lanisnik Rizner, *Steroids* **2005**, *70*, 626–635.
- [33] A.-M. Hoffrén, C. M. Murray, R. D. Hoffmann, *Curr. Pharm. Des.* **2001**, *7*, 547–566.
- [34] a) J. F. Couture, K. P. de Jesus-Tran, A. M. Roy, L. Cantin, P. L. Cote, P. Legend, V. Luu-The, F. Labrie, R. Breton, *Protein Sci.* **2005**, *14*, 1485–1497; b) M. Mazumdar, M. Zhou, D.-W. Zhu, A. Azzi, S.-X. Lin, *Cryst. Growth Des.* **2007**, *7*, 2206–2212; c) A. Hara, T. Nakayama, M. Nakagawa, Y. Inoue, H. Tanabe, H. Sawada, *J. Biochem.* **1987**, *102*, 1585–1592.
- [35] Discovery Studio 1.7, Accelrys Inc., 10188 Telesis Court, Suite 100 San Diego, CA 92121 (USA).
- [36] Insight II version 2005, Accelrys Inc., 10188 Telesis Court, Suite 100 San Diego, CA 92121 (USA).
- [37] M. L. Verdonk, J. C. Cole, M. J. Hartshorn, C. W. Murray, R. D. Taylor, *Proteins Struct. Funct. Genet.* **2003**, *52*, 609–623.
- [38] H. M. Berman, J. Westbrook, Z. Feng, G. Gilliland, T. N. Bhat, H. Weissig, I. N. Shindyalov, P. E. Bourne, *Nucleic Acids Res.* **2000**, *28*, 235–242.
- [39] E. Lindahl, B. Hess, D. van der Spoel, *J. Mol. Model.* **2001**, *7*, 306–317.
- [40] A. N. Jain, *J. Comput.-Aided Mol. Des.* **2000**, *14*, 199–213.
- [41] Sybyl version 7.3, Tripos Inc., St. Louis, MO (USA).
- [42] R. D. Cramer III, D. E. Patterson, J. D. Bunce, *J. Am. Chem. Soc.* **1988**, *110*, 5959–5967.
- [43] W. L. DeLano, The PyMOL Molecular Graphics System, **2002**, DeLano Scientific, Palo Alto, CA (USA).
- [44] A. W. Schüttelkopf, D. M. F. van Aalten, *Acta Crystallogr. Sect. D* **2004**, *60*, 1355–1363.
- [45] B. Hess, H. Bekker, H. J. C. Berendsen, J. G. E. M. Fraaije, *J. Comput. Chem.* **1997**, *18*, 1463–1472.
- [46] QSAR and CoMFA Manual, Sybyl version 7.3, Tripos Inc., St. Louis, MO (USA).

Received: September 26, 2007

Revised: December 5, 2007

Published online on January 25, 2008